Heliyon 10 (2024) e37530

Contents lists available at ScienceDirect

Heliyon

journal homepage: www.cell.com/heliyon

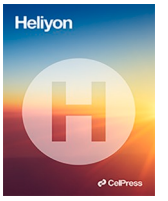

Research article

Influence of photosynthetic active radiation on sap flow dynamics across forest succession stages in Dinghushan subtropical forest ecosystem

Jianqiang Huang [a,b,d,1], Fasih Ullah Haider [a,b,d,1], Wanxuan Huang [a,b,c], Shizhong Liu [a,b,d], Brian Njoroge Mwangi [a,b,c], Vincent Suba [a,b,c], Lindsay Sikuku [a,b,c], Xuli Tang [a,b,d], Qianmei Zhang [a,b,d,**], Guowei Chu [a,e], Deqiang Zhang [a,b,d], Juxiu Liu [a,b,d], Ze Meng [a,b,d], Dennis Otieno [e], Yuelin Li [a,b,c,d,*]

[a] National Ecological Science Data Center Guangdong Branch, South China Botanical Garden, Chinese Academy of Sciences, Guangzhou, 510650, China
[b] Guangdong Provincial Key Laboratory of Applied Botany, South China Botanical Garden, Chinese Academy of Sciences, Guangzhou, 510650, China
[c] University of Chinese Academy of Sciences, Beijing, 100039, China
[d] South China National Botanical Garden, Guangzhou, 510650, China
[e] Jaramogi Oginga Odinga University of Science & Technology, 210-40601, Bondo, Kenya

ARTICLE INFO

Keywords:
Forest succession
Sap flow
Environment factor
Soil water content

ABSTRACT

With the intensification of global change, forests are subjected to varying degrees of drought or high-temperature stress, which has an indelible impact on the growth of trees. However, knowledge on the response of sap flow to environmental changes in different types of forests is still rare, especially in China's subtropical forest ecosystem. Consequently, studying how different tree species regulate their sap flow in response to shifting environmental conditions is essential for understanding forest transpiration, water use efficiency, and drought stress resilience. Therefore, this study aimed to investigate the sap flow dynamics of seven tree species in five forest plots, i.e., pine forest (PF), two types of mixed conifer-broadleaf forests (MF1+MF2), monsoon evergreen broadleaved forest (MEBF), and montane monsoonal evergreen broad-leaf forest (MOBF) at Dinghushan National Reserve in Southern China, using the heat dissipation probe technique and synchronous environmental factor recordings. Results demonstrated a significant influence of photosynthetic active radiation (PAR) on sap flow across all tree species, with mean PAR values ranging from over 1200 to 425 μmol m^{-2} s^{-1}, establishing it as the principal driving factor. This observation underscores the heightened responsiveness or sensitivity of tree species to variations in PAR as the forest undergoes development and maturation. The correlation between vapor pressure deficit (VPD) and tree sap flow decreased as succession

* Corresponding author. National Ecological Science Data Center Guangdong Branch, South China Botanical Garden, Chinese Academy of Sciences, Guangzhou, 510650, China.
** Corresponding author. National Ecological Science Data Center Guangdong Branch, South China Botanical Garden, Chinese Academy of Sciences, Guangzhou, 510650, China.
E-mail addresses: zqm@scbg.ac.cn (Q. Zhang), yuelin@scib.ac.cn (Y. Li).
[1] Contribute equally.

https://doi.org/10.1016/j.heliyon.2024.e37530
Received 17 January 2024; Received in revised form 26 August 2024; Accepted 4 September 2024
Available online 6 September 2024

progressed. Moreover, the influence of soil water content (SWC) on sap flow stability against environmental changes increased. Similar patterns were also found between the two MF, with MF-2 displaying ecological characteristics and environmental conditions more closely aligned with those of the late-successional MEBF. The study reveals the intricate relationship between environmental factors and sap flow regulation in tree species within a subtropical forest ecosystem. Addressing a comparative gap in sap flow correlation among dominant tree species at Dinghushan, it establishes a hydro-physiological foundation for understanding tree species substitution during forest succession. The results provide key insights for forest management and climate-related research. Future studies should delve into the long-term implications of observed sap flow dynamics, exploring their impact on tree species adaptability amid ongoing environmental changes.

1. Introduction

Forests are crucial in the global carbon (C), water, and nutrient cycles, significantly influencing many ecological processes [1]. These ecosystems exchange more water and C with the atmosphere than any other biome, considerably impacting the global climate [2]. The high water consumption of trees plays a crucial role in the hydrological cycle of ecosystems [1]. Water cycles are strongly affected by the increasing frequency and intensity of drought events [3]. Global warming exacerbates drought events, significantly impacting forest ecosystems' geographical distribution patterns, community structure, and composition, including tree growth and physiological characteristics [4]. Drought stress reduces tree diameter growth and biomass accumulation, stomatal conductance, photosynthesis activity, transpiration rate, and water use efficiency [5,6]. Hence, it is critical to understand the regulatory mechanisms by which trees' water use responds to climatic variations, determining the environmental stability of forest water consumption.

Various methods are available to quantify tree water use, including eddy covariance measurements [7], models [8], remote sensing techniques [9], and sap flow measurements [10] Among these, the thermal dissipation probe (TDP) technique is widely used to quantify forest transpiration [11,12]. Monitoring trunk sap flow provides a reliable and reproducible perspective of tree water uses at long time scales, helping us to understand trees' responses to the external environment and prevent their mortality due to climate change [13]. Several environmental conditions influence the rates of transpiration and sap flow in plants. As VPD increases, transpiration and sap flow initially rise due to greater atmospheric demand for water vapor. This trend continues until a species-specific threshold is reached. Beyond this point, trees begin to close their stomata to prevent excessive water loss, which can lead to a decline in transpiration and sap flow. Stomatal regulation is also influenced by intrinsic physiological traits, which varies among species. Isohydric species typically maintain stable water potential by closing their stomata [57], while anisohydric species exhibit more flexible stomatal behavior to optimize gas exchange under changing environmental conditions [58]. Increased photosynthetic active radiation (PAR) boosts photosynthesis rates, requiring higher CO_2 absorption [59]. To intake more CO_2, plants open their stomata, which in turn increases transpiration and water movement from roots to leaves, though plants carefully regulate their stomatal opening to balance CO_2 intake with water loss [60].

Although VPD, integrating temperature and relative humidity [14], is a primary factor affecting transpiration and sap production, other factors such as soil moisture [15], wind speed [16], and atmospheric CO_2 concentration also play crucial roles [17]. Extreme temperatures, whether very high or freezing, further affect these processes. As VPD increases, transpiration and sap flow initially rise due to greater atmospheric demand for water vapor [14]. This trend continues until a species-specific threshold is reached. Beyond this point, trees begin to close their stomata to prevent excessive water loss, which can lead to a decline in transpiration and sap flow [15]. Higher atmospheric CO_2 levels reduce stomatal conductance, thereby potentially slowing plant transpiration, though the relationship is complex and species-dependent. Understanding species-specific responses to these environmental conditions is essential for assessing potential species extinction and forest dynamics under global change [18,19]. In recent decades, Southern China has experienced rising atmospheric temperatures and changing rainfall patterns, leading to more frequent and severe droughts, decreased soil water content, and increased atmospheric water vapor pressure deficits [20–22]. Forests with a subtropical monsoon climate are susceptible to climate change due to the significant impact of changing environmental conditions on sap flow dynamics [9,10]. Water supply and atmospheric demand are affected by variations in rainfall patterns, temperature, and humidity [23]. These ecosystems are disrupted by climate change, which impacts water movement and tree physiology [24]. Therefore, comparative studies of the tree hydraulics of different subtropical forest species are vital.

Depending on the stage of forest succession, different tree species react differently to water VPD [3]. Because they have less access to water and less evolved water conservation strategies, early successional stages are more sensitive to VPD. This increases transpiration rates in drier conditions and more prominent stomatal closure. Tree species grow deep roots and better water-use techniques as succession advances, which lessens the sensitivity of those species to VPD [12]. In mature ecosystems, sap flow dynamics are primarily regulated by external conditions, particularly light radiation [19]. Trees adjust their crown structure to maximize light absorption, which in turn affects transpiration and sap flow. Additionally, photosynthetic activity influences transpiration and sap flow through stomatal regulation and CO_2 uptake while preserving resources like soil moisture and maintaining optimal temperature conditions [25,26]. Altitude variations in mountainous areas impact tree physiology, particularly sap flow dynamics, through changes in temperature, air pressure, and water availability. Higher altitudes can reduce sap flow due to lower temperatures, decreased air pressure, and changing soil moisture [27,28]. Because of different strategies of stomatal regulation (isohydric vs anisohydric), certain species exhibit enhanced sap flow rates, complicating the relationship between altitude and sap flow. Species composition and environmental factors,

especially climatic variables that change with altitude, influence the way sap flow responds to these conditions.

Previous studies have examined tree hydraulics parameters such as sap flow density, whole tree transpiration, and canopy stomatal conductance of some dominant tree species in certain forest types and their relationship with environmental factors [13,29]. However, there is a lack of comparative research examining the water usage of identical tree species inhabiting a comprehensive successional sequence, ranging from pioneer forests such as pine forests (PF) through mid-successional forests like mixed conifer-broadleaf forests (MF), to late-successional forests, including monsoon evergreen broad-leaved forests (MEBF) in the Dinghushan Mountains, China. Moreover, the knowledge about the water use of montane evergreen broad-leaved forest (MOBF) tree species formed under low temperatures and intense light at high altitudes has yet to be reported. Therefore, conducting in-depth sap flow measurement studies on the dominant tree species of different forest types in the successional series is essential.

Therefore, this study investigates the variations in water use during the growth and decline of species across forests at distinct successional stages, offering valuable insights into forest dynamics in the context of global change. Employing the TDP technique, we monitored trunk sap flow within five sample plots across four forest types in the Dinghushan Mountain region. The primary objectives of this study were to 1) identify the critical environmental factors influencing water usage in tree species across varying successional forests, 2) assess the differential responsiveness of tree species to environmental changes at different successional stages, and 3) examine the impact of altitude on water usage in identical or similar forest type tree species. We hypothesized that: 1) water vapor pressure deficit is the primary environmental driver, with its impact varying across successional stages; 2) as succession advances, sap flow dynamics in tree species become more sensitive to light radiation, while demonstrating greater conservation in response to other environmental influences; and 3) SWC plays a critical role in mediating the ecological advancement of forests from mid to late succession.

2. Materials and methods

2.1. Description of the experimental sites

The research was conducted at Dinghushan National Nature Reserve in western Guangdong Province (23°09′21'' - 23°11′30''N, 112°30′39'' - 112°33′41″ E), China (Fig. S1). Dinghushan forest reserve covers a total area of 1155 ha and is characterized by a typical subtropical humid monsoon climate with an average annual temperature and rainfall of 20.9 °C and 1956 mm, respectively [20,30]. Due to environmental variations caused by differences in altitude, various subtropical forest types occur at different altitudes on Dinghushan Mountain. Gully rainforests have developed on the slopes of both sides of the river valley at altitudes of 50–150 m. Pine forests (PF) are found in hilly areas below 300m, mixed conifer-broadleaf forests (MF) are distributed at heights of 100–450 m, and monsoon evergreen broad-leaved forests (MEBF) are the regional, zonal forest vegetation type, distributed at altitudes of 30–400 m. Montane evergreen broad-leaved forests (MOBF) are located on hillsides above 500 m [31,32]. Among these forest types in Dinghushan Mountain, PF, MF, and MEBF are typical monsoon evergreen succession series vegetation. In contrast, MEBF and MOBF constitute specific natural vegetation types of subtropical evergreen broad-leaved forests at different altitudes [30,33]. Furthermore, due to complex ecological community interactions, similarly mixed forests have formed at different altitudes, with those located at lower altitudes being named MF-1 and those at higher altitudes being named MF-2. Data on altitude, forest age, temperature, soil type, and average diameter at breast height for the various tree species in their respective sites are provided in Table 1.

2.2. Measurements

2.2.1. Plot survey

Five experimental plots with similar aspects and slopes were selected as trunk sap flow plots in the above five forest plots (Fig. S1, Table 1, Table S1). Each of the 5 (PF, MF-1, MF-2, MEBF, and MOBF) trunk sap flow plot was sub-divided into six plots with dimensions of 10 m × 10 m of smaller plots, except MEBF, which was sub-divided into 12 sub-plots. A vegetation survey was conducted for each sub-plot, with the leading survey indicators including species composition, tree height, diameter at breast height, crown width, and the coordinates of the trees within the sample square. At least three trees for each species were selected as sample trees with straight

Table 1
Brief introduction of study sites.

	PF	MF-1	MF-2	MEBF	MOBF
Altitude (m)	60	30	320	215	600
Succession stage	primary	Intermediate	intermediate	late	late
Stand age (a)	70	70	70	400	100
Tree canopy cover (%)	70–80	70–80	80–90	80–90	80–90
Main tree species	*P. massoniana*	*P. massoniana* *S. superba* *C. chinensis* *M. chinensis*		*S. superba* *C. chinensis* *M. chinensis*	*M. breviflora* *M. seguinii* *R. henryi*
Soil type	red soil	red soil	red soil	red soil	yellow soil

Note: PF, MF, MEBF, and MOBF refer to pine forest, mixed conifer-broadleaf forest, monsoon evergreen broadleaved forest, and montane monsoonal evergreen broad-leaf forest respectively.

trunks, free from pests and diseases, in good growth condition, and with relatively little canopy shading from the surrounding vegetation. Based on the tree survey data, seven dominant tree species; *Pinus massoniana* L., *Schima superba* L., *Machilus chinensis* L., *Castanopsis chinensis* L., *Machilus breviflora* L., *Myrsine seguinii* L., and *Rhododendron henryi* L. were selected for continuous measurement of trunk sap flow.

2.2.2. Microclimate monitoring

Monitoring systems were established at five sampling sites to measure microclimate. Soil moisture sensors (CS616, Campbell Scientific, Utah, USA) were placed at a depth of 20 cm in each plot. The soil was stratified to maintain its natural state after digging and filling the pits. Observation points for atmospheric temperature and humidity (HMP155A, Vaisala, Helsinki, Finland) and photosynthetically active radiation (PQS1, Kipp & Zonen, Delft, Netherlands) were set up on a flat field surrounding the sample plot. Temperature and humidity sensors were mounted at a height of 2 m, while the radiation sensor was installed horizontally in an open location with a height of 3 m to ensure that its sensing surface was not obstructed. All sensors were connected to a data logger (CR1000, Campbell Scientific, Utah, USA), and mean values were calculated and recorded every 30 min.

The Vapor Pressure Deficit (VPD) indicator reflects the combined effect of air temperature and relative humidity. The saturated water vapor pressure, denoted as $e_s(T)$, was calculated using Equation (1):

$$e_s(T) = a \times \exp^{\frac{bT}{T+c}} \tag{1}$$

The VPD was then determined using Equation (2) [29,34]:

$$\mathrm{VPD} = e_s(T) - e_a = e_s(T) \times (1 - \mathrm{RH}) \tag{2}$$

where, the formula $e_s(T)$ represents the saturated water vapor pressure (kPa) at the temperature of T(°C), e_a was the actual water vapor pressure (kPa). Parameters a, b, and c were equivalent to 0.611 kPa, 17.502, and 240.97 °C, respectively. RH was the relative humidity, and VPD was the vapor pressure deficit (kPa) between the leaves and the air.

2.2.3. Sap flow measurements

Sap flow measurements were conducted using the Granier heat dissipation probe method from August 2019 to March 2020. Due to variations in installation times, the commencement dates for data collection differed across sites. Technical issues resulted in data loss at specific locations; consequently, data collection at the MEBF site commenced in October 2019, whereas it concluded at the PF site in October 2019. The sensor, comprising a pair of 20 mm-long probes, was installed at a height of 1.3 m on the northern side of the tree trunk. For large diameter tree classes, probes were set at sapwood depths of 0–20 mm and 20–40 mm. To install the probes, two holes were drilled 10 cm apart at breast height on the sample tree using an electric drill. An aluminum tube was inserted into the hole for protection and optimal heat conduction, followed by the insertion of a TDP pair. Silicone grease was applied to prevent friction damage, rusting, and to ensure uniform heat distribution to the tree trunk. To avoid erosion by rainwater and minimize the influence of sunlight, the probes were covered with a foam box and wrapped with radiation protection film. The upper probe was continuously heated (0.2W) with a 12V DC voltage, while the lower probe served as a reference. The thermoelectric potential between the two probes was recorded and stored automatically using a data collector (CR1000, Campbell Scientific, Utah, USA) at one reading every 10 s, with the average value stored every 30 min. Sap density was calculated from the thermoelectric potential using an empirical formula (Equation (3)) developed by Granier [35] based on research on various tree species:

$$J_s = 119 \times \left(\frac{\Delta T_m - \Delta T}{\Delta T}\right)^{1.231} \tag{3}$$

Where ΔT_m was the maximum day-night temperature difference between the upper and lower probes, ΔT was the instantaneous temperature difference and J_s was the instantaneous sap flux density ($g \cdot H_2O \cdot m^{-2} \cdot s^{-1}$).

2.2.4. Average stomatal conductance

Since it was difficult to obtain the leaf area data of the monitored trees, assuming that the sap flow density is equal to canopy transpiration, the stomatal canopy conductance (g, $mmol \cdot m^{-2} \cdot s^{-1}$) was calculated using the following formula (Equation (4)) [36]:

$$g = \frac{J_s}{\mathrm{VPD}} \tag{4}$$

2.2.5. Time lag and inflection points measurement

Time lag measurement was analyzed by cross-correlation, which was computed with the stats package in R from the codes like: 'ccf (data$sapflow, data$TA, lag.max = 4) %>% with (lag[which.max(abs(acf))])'. Inflection points were measured by quadratic fit with codes such as 'lm(sap flow ~ poly(vpd, 2, raw = T), data = mydata)'.

Normalized hysteresis curves between half-hourly sap flux density and environmental factors also been analyzed using method from Pappas [37].

2.2.6. Tree species' light saturation point using unary quadratic fit

We define the light saturation point in plants as the intensity of light (photosynthetically active radiation or PAR) at which

photosynthesis reaches its maximum rate and does not increase further with additional light, using a unary quadratic fit (Equation (5)):

$$y = ax^2 + bx + c \quad (5)$$

Where y was sap flow density and x was environment factor. Then $-b/2a$ would be the light saturation point.

2.3. Data processing, statistical analysis, and graphing

Baseliner 4.0 software [38] was used for the calibration and quality control of the raw trunk sap flow data. R 3.5.3 software [39] was used to analyze, process, graph flow, and environmental data. Cross-correlation was used for time lag analysis using the ccf function in the stats package, step function in the same package was used for multiple stepwise regression analysis. The "pcor" function from ppcor package was used to analyze partial correlation. Statistical parameters were obtained using the 'stargazer' function from the stargazer package [40]. Statistical smoothing of climate factors shown in Fig. 1 is conducted by Generalized Additive Models using ggplot2: 'geom_smooth (method = 'gam')'. All figures were made using the ggplot2 package and its derivative packages.

3. Results

3.1. Environmental variability of the four forest types

The mean T, PAR, and VPD values recorded for the five measurement plots (Fig. S1) during the experimental period are shown in Fig. 1. During the research period, the mean PAR and VPD values decreased from PF to MF to MEBF. At different elevations, the mean value of PAR increased by 8.2 %, while the mean value of VPD decreased by 19.8 % in MF at a high elevation (MF-2) compared with a low one (MF-1). The mean value of VPD in MOBF was the lowest among all sample plots, while PAR was high, 90.4 % and 321.8 % of that in MEBF, respectively (Table 2).

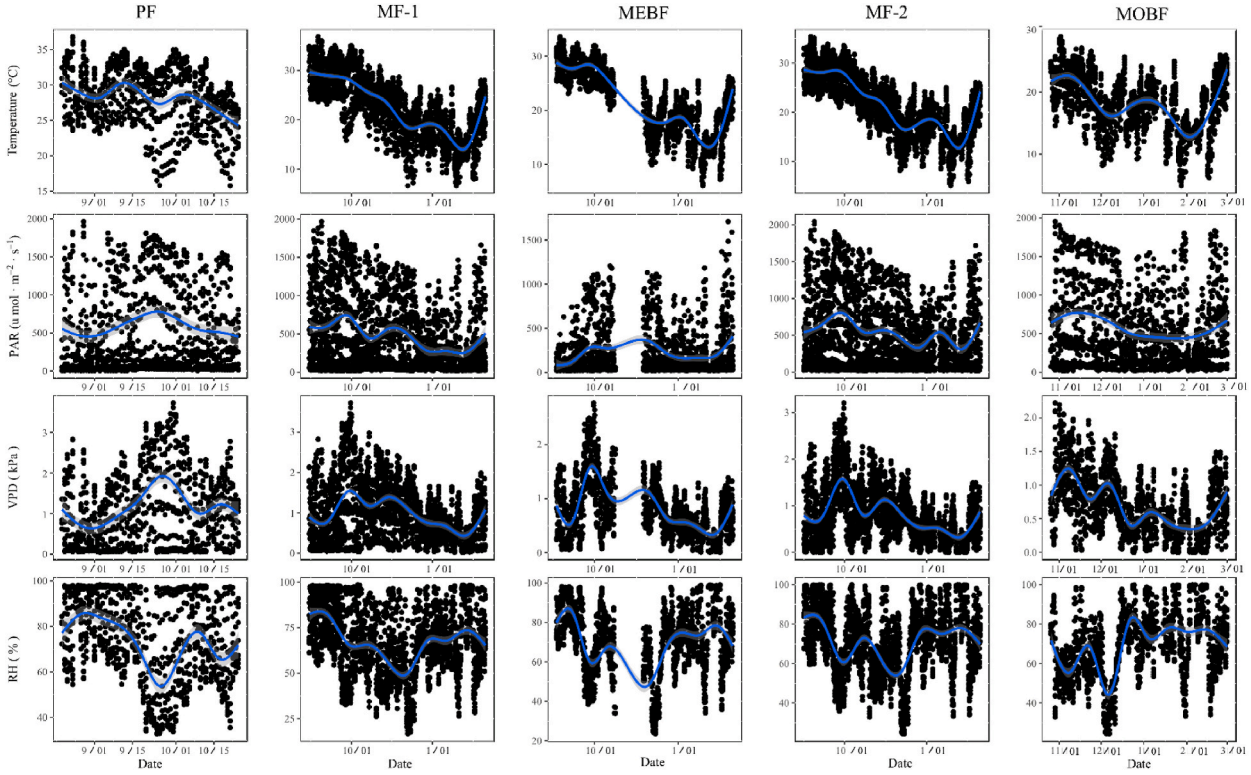

Fig. 1. Comparisons of climate factors between sites during the study period. The hourly average value of climate factors is shown in the figure, where the blue line shows the statistical smoother. Each horizontal row corresponds to an environmental factor, from top to bottom, temperature, PAR, VPD, and RH. Each vertical column corresponds to a forest type, from left to right, PF, MF-1, MEBF, MF-2 and MOBF, respectively. PAR = photosynthetic active radiation; RH = relative humidity; VPD = vapor pressure deficit; PF = pine forest; MF = mixed conifer-broadleaf forest; MEBF = monsoon evergreen broadleaved forest; MOBF = montane monsoonal evergreen broad-leaf forest.

Table 2
Diurnal variation of climate data in five study sites during the measuring period.

	PAR (umol m^{-2} s^{-1})	Temperature (°C)	RH (%)	VPD (kPa)
PF	581.6 ± 548.2	28.2 ± 4	73.2 ± 18.3	1.15 ± 0.89
MF-1	450.8 ± 475.1	22.6 ± 6.4	68.6 ± 19.3	0.95 ± 0.72
MF-2	487.8 ± 480.0	21.4 ± 6.2	71.6 ± 17.2	0.79 ± 0.59
MEBF	167.4 ± 256.3	21.6 ± 6.0	72.5 ± 17.5	0.75 ± 0.54
MOBF	538.7 ± 502.5	18.0 ± 4.6	69.6 ± 17.6	0.68 ± 0.46

Note: Data in the table were presented as mean ± standard deviation. PAR = photosynthetic active radiation; RH = relative humidity; VPD = vapor pressure deficit; PF = pine forest; MF = mixed conifer-broadleaf forest; MEBF = monsoon evergreen broadleaved forest; MOBF = montane monsoonal evergreen broad-leaf forest.

3.2. Time lags and inflection points of sap flow response to environmental factors

Cross-correlation analysis was applied between environmental factors and the sap flow density of each dominant tree species in each plot to study the time-lag relationship (Table 3). Time dynamics of sap flow density of *P. massoniana* species in PF plot lagged behind PAR by 1 h; *P. massoniana* and *S. superba* lagged behind PAR in plot MF-1 by1 hour, while *C. chinensis* and *M. chinensis* had a non-hysteretic relationship with RH and VPD by1 hour. There was a non-significant time-lag relationship between the sap flow density of each dominant tree species and environmental factors in the MF-2.

In MEBF, no time-lag relationship was observed between sap flow and PAR, while for RH, *T*, and VPD, there was a 1–2 h (s) time lag in sap flow. The daily dynamics of the sap flow density of the four dominant tree species in MOBF all lag behind PAR by 2 h but with a non-significant time-lag relationship with other environmental factors.

Unary quadratic fitting between flow density and PAR and VPD is shown in Table 4. *P. massoniana* was not restricted by PAR in PF, MF-1, and MF-2. The light saturation points of *S. superba* and *C. chinensis* in two MF plots were high (more than 1200 μmol·m^{-2}·s^{-1}), while those of all tree species in the MEBF were low, with *M. chinensis* being the lowest (400 μmol·m^{-2}·s^{-1}). The dominant tree species of MOBF were not limited by light, with the perspective of a straightly fitting line.

The quadratic adjustment between the sap flow and the VPD showed that the VPD saturation point of *S. superba* in MF-1, MF-2, and MEBF was higher than that of *C. chinensis*. On the other hand, *M. chinensis* had the lowest saturation point in MF-1 and MEBF. The *a* values of species in MOBF were positive, and -b/2a values were all negative except for *R. henryi* (0.11 kPa). Given that the mean VPD in MOBF was 0.68 kPa, the limitation imposed by VPD was not severe for this site.

3.3. Partial correlation between sap flow and microclimate

Since the hydrothermal conditions of MF-2 were more like those of MEBF, MF-1 was used as a representative of mixed forest to compare the common species sap flow response to environmental factors among PF, MF-1, and MEBF (Fig. 2). The sap flow of all tree species was strongly partially correlated with VPD, and this correlation was decreased in the next successional forest type. Correspondingly, the correlation between sap flow and PAR was increased and was the primary environmental driver in *C. chinensis* and *M. chinensis*. On the other hand, there was not a strong correlation between sap flow and SWC for all tree species. However, they did increase in the next successional forest except for *M. chinensis*, though the resultant R^2-values remained very low, except for *P. massoniana*.

Table 3
Time lags between sap flow density and environmental factors occurred in the dominant tree species at different study sites.

Site names	Species	PAR	RH	*T*	VPD
PF	*P. massoniana*	1	0	0	−1
MF-1	*P. massoniana*	1	0	0	0
	S. superba	1	0	0	0
	C. chinensis	0	0	−1	−1
	M. chinensis	0	0	−1	−1
MF-2	*P. massoniana*	0	0	0	0
	S. superba	0	0	0	0
	C. chinensis	0	0	0	0
	M. chinensis	0	0	0	0
MEBF	*S. superba*	0	−2	−1	−2
	C. chinensis	0	−2	−1	−1
	M. chinensis	0	−2	−1	−1
MOBF	*M. breviflora*	2	0	0	0
	M. seguinii	2	0	0	0
	R. henryi	2	0	0	0

Note: The unit in the table is hour, in which a positive value means that the sap flow lags the environmental factor, and the negative value means the sap flow was ahead of the environmental factor. PAR = photosynthetic active radiation; RH = relative humidity; VPD = vapor pressure deficit; PF = pine forest; MF = mixed conifer-broadleaf forest; MEBF = monsoon evergreen broadleaved forest; MOBF = montane monsoonal evergreen broad-leaf forest.

Table 4
Quadratic model parameters between sap flow density and PAR and VPD for the dominant tree species at different study sites.

Site	Species	$J_s = a\,x^2 + b\,x + c$							
		x = PAR(umol·m^{-2}·s^{-1})				x = VPD(kPa)			
		a	*b*	-b/2a	R^2	*a*	*b*	-b/2a	R^2
PF	*P. massoniana*	−0.00000***	0.016**	–	0.532	−2.780***	14.330***	2.58	0.783
MF-1	*P. massoniana*	0.00000***	0.005**	–	0.495	−0.039	7.424***	95.18	0.675
	S. superba	−0.00001***	0.029***	1450	0.652	−3.514***	19.554***	2.78	0.713
	C. chinensis	−0.00001***	0.024***	1200	0.744	−2.752***	15.134***	2.75	0.711
	M. chinensis	−0.00001***	0.032***	1600	0.68	−3.908***	19.129***	2.45	0.609
MF-2	*P. massoniana*	0.00000***	0.010***	–	0.665	−0.413**	12.250***	14.83	0.766
	S. superba	−0.00001***	0.026***	1300	0.774	−2.897***	16.807***	2.90	0.602
	C. chinensis	−0.00001***	0.028***	1400	0.787	−3.989***	18.027***	2.26	0.551
	M. chinensis	0.00000**	0.013***	–	0.579	0.887**	12.890***	−7.27	0.668
MEBF	*S. superba*	−0.00002***	0.027***	675	0.257	−4.163***	15.034***	1.81	0.25
	C. chinensis	−0.00001***	0.022***	1100	0.462	−2.461***	9.477***	1.93	0.379
	M. chinensis	−0.0001***	0.080***	400	0.399	−10.123**	30.162***	1.49	0.253
MOBF	*M. breviflora*	0.00000*	0.003***	–	0.238	1.502***	6.719***	−2.24	0.732
	M. seguinii	0.00000	0.003***	–	0.207	2.884***	2.326***	−0.40	0.589
	R. henryi	0.00000***	0.0004	–	0.149	2.710***	−0.599***	0.11	0.741

Note: *$p < 0.1$; **$p < 0.05$, ***$p < 0.01$. J_s represents the sap flow density, a quadratic fit was made to the two kinds of x. On the left side, x represents PAR, and the x on right side represents VPD. *a*, *b* were the fitting parameters, from which -b/2a was calculated. PAR = photosynthetic active radiation; VPD = vapor pressure deficit; PF = pine forest; MF = mixed conifer-broadleaf forest; MEBF = monsoon evergreen broadleaved forest; MOBF = montane monsoonal evergreen broad-leaf forest.

The sap flow of tree species was also strongly influenced by VPD at MF at different altitudes (Fig. 3). Except for *M. chinensis*, the partial correlations between sap flow and VPD and SWC in *P. massoniana*, *S. superba*, and *C. chinensis* all decreased at high altitudes. In contrast, the correlation between sap flow and PAR was increased, with *S. superba* and *C. chinensis* being more affected by PAR than VPD at high altitudes. For evergreen broad-leaf forests on different elevation gradients, the sap flow of dominant tree species in MEBF showed a stronger correlation with PAR. In MOBF, the predominant driving factor for sap flow in the dominant tree species was VPD (Fig. 4).

3.4. Multivariate regression between sap flow and microclimate

In the multivariate regression model analysis (Table 5), the dominant environmental factor affecting the sap flow of common species present in PF, MF-1, and MEBF forests without exception changed from VPD to SWC in the following successional sequence. Comparing MF at different elevations and thus different environmental conditions (MF-1 and MF-2), it was found that the dominant environmental factor of *P. massoniana* sap flow was SWC ($p < 0.01$) at both elevation gradients. However, higher altitude decreased the weight of VPD effects on the sap flow of all dominant tree species. On the other hand, SWC was the dominant environmental influence factor ($p < 0.01$) for the sap flow of all dominant species in evergreen broad-leaf forests at different elevations (MEBF and MOBF). The *M. breviflora* sap flow data had non-significant correlation with SWC, and the model residuals were large, which might be caused by systematic errors.

4. Discussions

4.1. Sensitivity of sap flow to environmental changes across forest succession stages

Photosynthetically active radiation (PAR) substantially impacted sap flow more than other weather conditions, exhibiting a decreasing trend across the three successional stages (PF to MF-1 to MEBF) (Fig. 1, Table 2). Conversely, the responses of sap flow to relative humidity (RH) and temperature (T) were inconsistent among forest types. The vapor pressure deficit (VPD) showed a downward trend, which we initially attributed to the prevalence of shade-tolerant trees in later successional stages [41]. However, further analysis suggests that elevation plays a more critical role, as MEBF is situated approximately 150 m higher than PF/MF-1, leading to lower temperatures and thus lower VPD. Additionally, canopy cover and structure could significantly influence these climate variables, with higher temperatures and VPD at PF compared to MF-1 at similar elevations. MF-1 was selected as the representative mixed forest type for further comparative analysis (Tables 1 and 2).

All tree species in this study exhibited synchronous or lagged responses to PAR (Table 3), suggesting that PAR was the primary driver for trunk sap flow [42]. Sap flow onset lagged behind PAR in early successional stages, while it was nearly simultaneous for light-loving species like *S. superba* in middle successional stages. Previous research has also shown a time lag effect of sap flow in response to light, similar to our findings. For example, Larch trunk sap flow in a Greater Khingan Mountains forest exhibited lagged responses to PAR [25], and sap flow in an artificial Poplar Forest on sandy land lagged behind solar radiation but led T, RH, and VPD [42]. As succession advanced, the time lag effect of sap flow in response to light decreased until it disappeared. MOBF, characterized by high light intensity and a similar vertical community structure to PF due to small tree size (Table S2), demonstrated a comparable sap

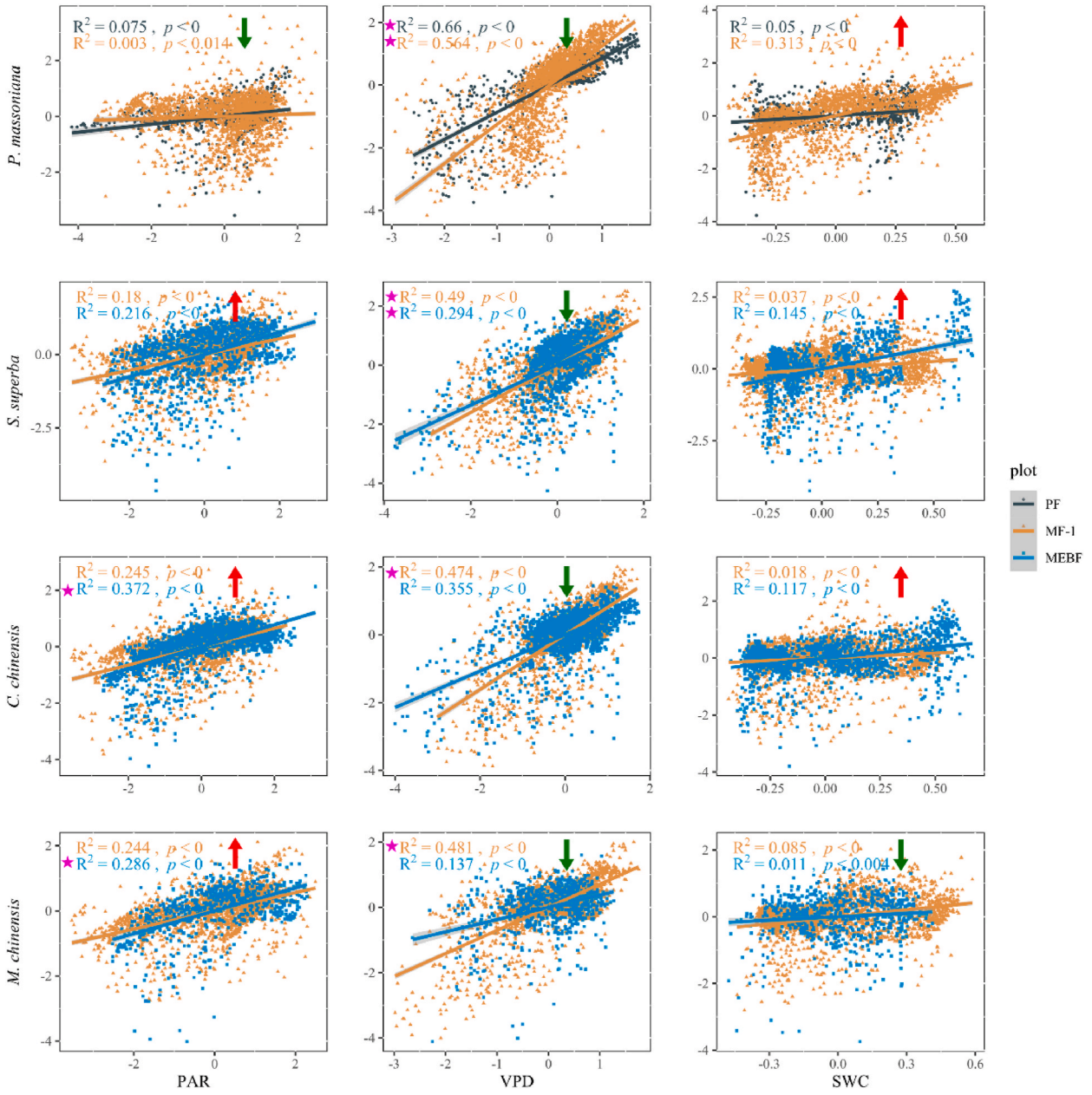

Fig. 2. Par-correlation between sap flux density and environmental factors at the PF, MF-1, and MEBF sites. Each horizontal row represents a tree species, each vertical column represents an environmental factor, and different colors indicate different sample sites. All variables, including *Js*, PAR, VPD, and SWC, were transformed using natural logarithm to eliminate the influence of statistical units. All horizontal and vertical coordinates are linear regression residuals of the corresponding environmental factors and sap flow of the tree species with the remaining environmental factors, respectively. The green down arrows to the right of each set of R^2 and *P* indicate a smaller partial correlation coefficient for the forest type below, while the red arrows indicate the opposite. The purple pentagram on the left side indicates that this environmental factor's partial correlation coefficient with the current tree species was the largest among all environmental factors. PAR = photosynthetic active radiation; VPD = vapor pressure deficit; SWC = soil water content; PF = pine forest; MF = mixed conifer-broadleaf forest; MEBF = monsoon evergreen broad-leaved forest.

flow response rate to light in early successional stages.

Our results were consistent with a study on the light saturation points of dominant tree species in Tiantong Mountain, located in Zhejiang Province, China, which demonstrated a decreasing trend as succession progressed [43]. In Dinghushan Mountain, *P. massoniana* exhibited a higher yet unsaturated light saturation point in PF and MF-1, while tree species like M. chinensis had lower PAR and VPD saturation points. It is important to note that PAR measurements were taken within the canopy, which can significantly

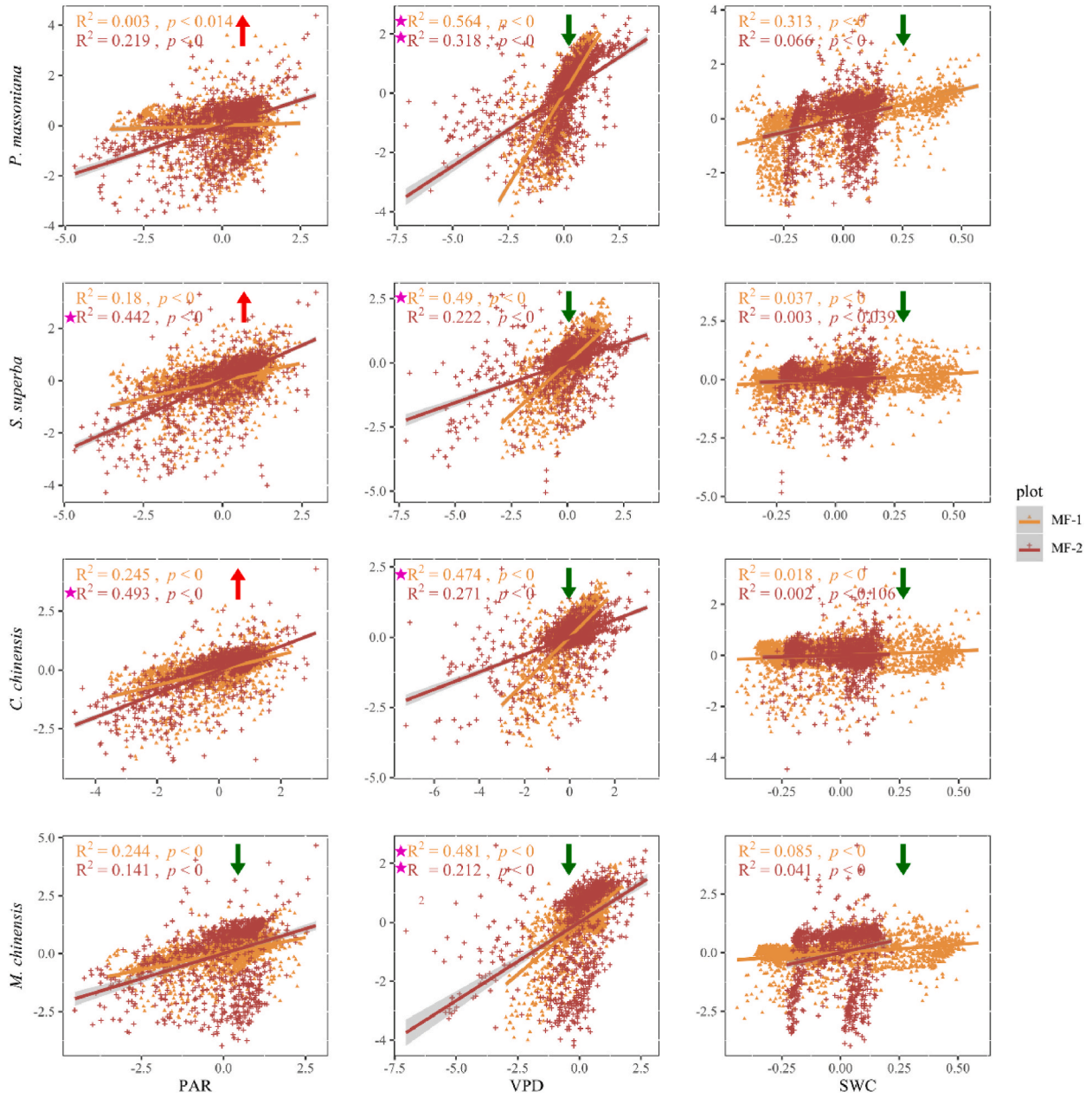

Fig. 3. Par-correlation between sap flux and environmental factors at two MF sites. Each horizontal row represents a tree species, each vertical column represents an environmental factor, and different colors indicate different sample sites. All variables, including *J*s, PAR, VPD, and SWC, were transformed using natural logarithm to eliminate the influence of statistical units. All horizontal and vertical coordinates are linear regression residuals of the corresponding environmental factors and sap flow of the tree species with the remaining environmental factors, respectively. The green down arrows to the right of each set of R^2 and *P* indicate a smaller partial correlation coefficient for the forest type below, while the red arrows indicate the opposite. The purple pentagram on the left side indicates that this environmental factor's partial correlation coefficient with the current tree species was the largest among all environmental factors. PAR = photosynthetic active radiation; VPD = vapor pressure deficit; SWC = soil water content; MEBF = monsoon evergreen broadleaved forest; MOBF = montane monsoonal evergreen broadleaf forest.

influence the values due to the canopy structure. Therefore, while our findings align with those of other studies, caution should be exercised when making direct comparisons. This suggests a higher PAR saturation point in MF-1 but reduced capacity in other physiological aspects, such as sap flow density and crown stomatal conductivity, potentially limiting growth and decreasing vital values [28,44]. MOBF species did not display distinct PAR and VPD saturation points, implying more restrained stomatal behavior, leading to slow and continuous water vapor exchange with the atmosphere.

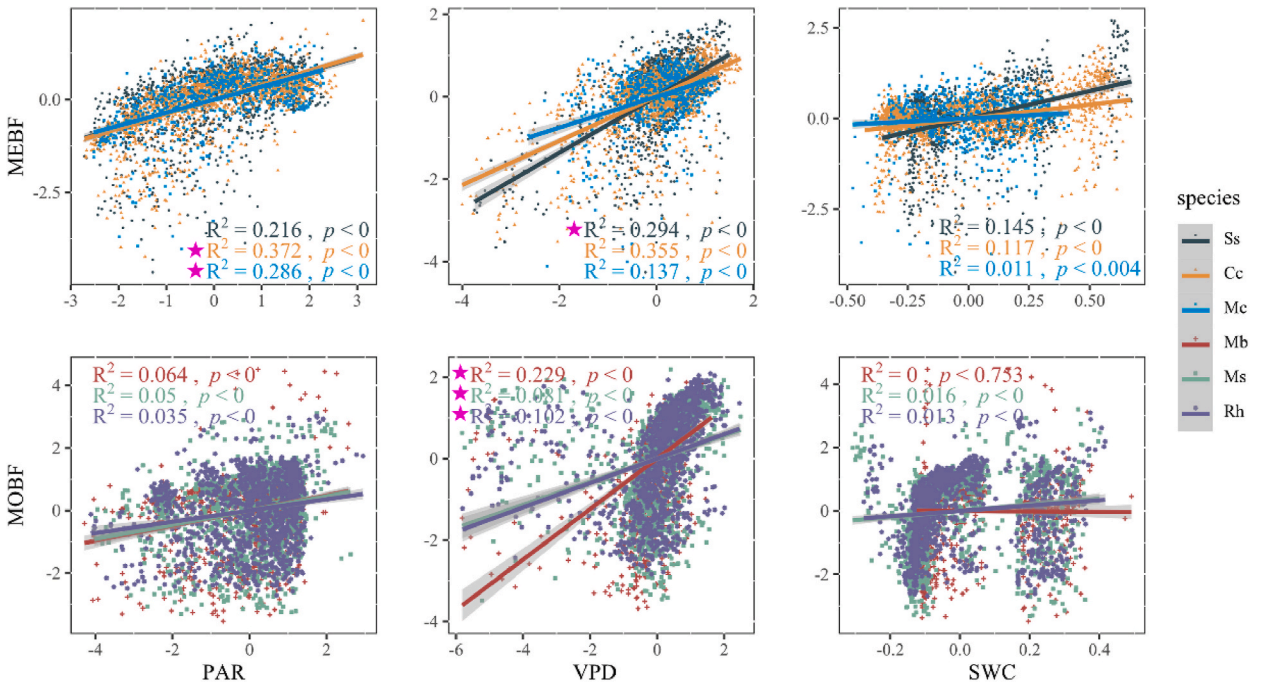

Fig. 4. Par-correlation between sap flux and environmental factors at the MEBF and MOBF sites. Each horizontal row represents a tree species, each vertical column represents an environmental factor, and different colors indicate different sample sites. All variables, including *Js*, PAR, VPD, and SWC, were transformed using natural logarithm to eliminate the influence of statistical units. All horizontal and vertical coordinates are linear regression residuals of the corresponding environmental factors and sap flow of the tree species with the remaining environmental factors, respectively. The green down arrows to the right of each set of R2 and P indicate a smaller partial correlation coefficient for the forest type below, while the red arrows indicate the opposite. The purple pentagram on the left side indicates that this environmental factor's partial correlation coefficient with the current tree species was the largest among all environmental factors. PAR = photosynthetic active radiation; VPD = vapor pressure deficit; SWC = soil water content; PF = pine forest; MF = mixed conifer-broadleaf forest; MEBF = monsoon evergreen broadleaved forest.

Table 5
Results of multiple regression models of sap flow density and environmental factors for tree species in different forests.

Plots			$\ln(Js) = \beta_1 \times \ln(VPD) + \beta_2 \times \ln(PAR) + \beta_3 \times \ln(SWC) + \alpha$						
			P. massoniana	*S. superba*	*C. chinensis*	*M. chinensis*	*M. breviflora*	*M. seguinii*	*R. henryi*
PF	β_1	(VPD)	**0.699*****	–	–	–	–	–	–
	β_2	(PAR)	0.236***	–	–	–	–	–	–
	β_3	(SWC)	0.114***	–	–	–	–	–	–
	R^2		0.725	–	–	–	–	–	–
MF-1	β_1	(VPD)	**0.660*****	**0.592*****	**0.568*****	**0.623*****	–	–	–
	β_2	(PAR)	0.182***	0.319***	0.349***	0.284***	–	–	–
	β_3	(SWC)	0.266***	0.082***	0.053***	0.134***	–	–	–
	R^2		0.682	0.695	0.693	0.707	–	–	–
MF-2	β_1	(VPD)	0.328***	0.341***	0.409***	0.353***	–	–	–
	β_2	(PAR)	**0.546*****	**0.580*****	**0.517*****	**0.384*****	–	–	–
	β_3	(SWC)	0.124***	−0.022	0.007	0.128***	–	–	–
	R^2		0.606	0.683	0.674	0.421	–	–	–
MEBF	β_1	(VPD)	–	0.275***	0.362***	0.258***	–	–	–
	β_2	(PAR)	–	**0.588*****	**0.514*****	**0.556*****	–	–	–
	β_3	(SWC)	–	0.406***	0.177**	0.236***	–	–	–
	R^2		–	0.488	0.447	0.413	–	–	–
MOBF	β_1	(VPD)	–	–	–	–	**0.422*****	**0.284*****	**0.368*****
	β_2	(PAR)	–	–	–	–	0.329***	0.254***	0.190***
	β_3	(SWC)	–	–	–	–	−0.088***	0.077**	0.011
	R^2		–	–	–	–	0.401	0.216	0.229

Note: *p < 0.1; **p < 0.05; ***p < 0.01; R-squared adjusted. The bolded coefficient represents the largest coefficient of sap flow density and each environmental factor in this tree species. PF = pine forest; MF = mixed conifer-broadleaf forest; MEBF = monsoon evergreen broadleaved forest; MOBF = montane monsoonal evergreen broad-leaf forest.

4.2. Sap flow response to microclimate at different successional stages

Numerous studies have highlighted that PAR is the primary environmental factor for regulating sap flow, especially in forest ecosystems [10,26,29,36,45]. However, sap flow responses to microclimate factors may vary between wet and dry or growing and non-growing seasons [12,29]. In our study, we observed a strong correlation between the sap flow of all tree species and VPD, which decreased as succession progressed (Fig. 5). As forests mature, trees often develop physiological adaptations such as greater fine root production [46,47], reducing their reliance on immediate atmospheric conditions and making them less sensitive to changes in VPD. This suggests that the influence of a single environmental factor on tree species may diminish with succession.

Additionally, prior research has primarily focused on the short-term temporal scale when examining the relationship between sap flow and environmental factors [48,49]. By comparing the sap flow relationship across different forest types, we discovered a weak partial correlation ($R^2 < 0.15$) between tree species' sap flow and SWC (Figs. 2–4). Indicating a weak direct association when other environmental variables like PAR and VPD were controlled for. Conversely, adjusting the contributions of multiple environmental variables simultaneously, the multivariate regression analysis demonstrated that SWC becomes a significant predictor in the later stages of forest succession (Table 5). This finding revealing a more substantial role for SWC in conjunction with other factors, suggests that the resistance of tree water transport function to environmental changes may increase over time, or trees may need to enhance their ecological resistance capacity to better adapt to the following succession sequence [30].

4.3. Successional versus altitude effects on sap flow within mid-successional forest

In this study, the distinctions between the mid-successional stages MF-1 and MF-2 are particularly noteworthy. Although both are categorized under the mid-successional stage, MF-2 shares a closer resemblance in environmental conditions (Table 1) and tree hydraulics (Table 4) to MEBF, a late-successional forest. This similarity suggests that MF-2, while still technically a mid-successional forest, exhibits ecological characteristics that are more advanced compared to MF-1.

When comparing the two MF forests (Fig. 3), the partial correlation between the sap flow of tree species in MF-2 and both VPD and SWC decreased, with VPD's influence on the sap flow of all dominant tree species reduced at MF-2, which aligns with the hydraulic changes across different successional forests (Table 4). However, the growth of *M. chinensis* in MF-2 was restricted, exhibiting smaller tree height and DBH than its MF-1 counterpart (Table 1). A possible explanation is that Dinghushan's MF-2 environment remains suitable for mixed forest species, with PAR and VPD conditions still needing to reach the saturation point for each dominant species (Table 4). Simultaneously, MF-2 had stronger solar radiation, which enabled other intermediate tree species to obtain better growth opportunities and occupy the living space of shade tree species like *M. chinensis*.

In our study, we noted that MF-1 and MF-2 were located at different elevations. This observation aligns with existing research that investigates elevation effects on tree hydrology. For instance, Obojes et al. [50] observed that short-term drought had minimal effects on *L. decidua* sap flow and plant growth in high-altitude areas in Northern Italy, resembling our observation that sap flow of tree species relied more on SWC in later succession stages. Moreover, Zhu et al. [51] noted decreased crown width and leaf water potential of high-altitude plants in mixed forests at varying elevations. We partially replicated these patterns in our study at MF-1 and MF-2, where the influence of elevation on tree hydrology appeared mediated by shifting environmental conditions rather than having a direct effect. These findings suggest that the comparison between MF-1 and MF-2 offers a unique perspective on ecological progression within the mid-successional stage. By examining these dynamics, we can gain deeper insights into forest succession and its implications for ecosystem management and resilience in adapting to global environmental shifts.

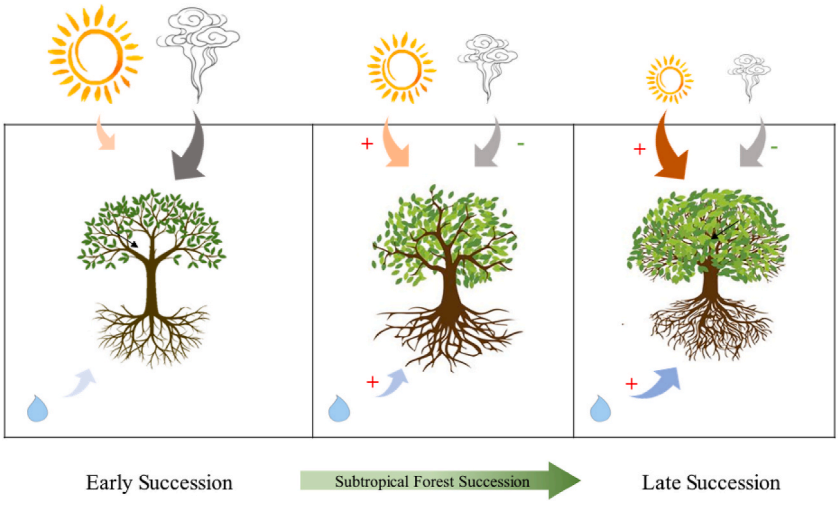

Fig. 5. Sap flow reacts to the environment in different succession stages and different elevations. Sun, vapor, and water droplets represent the effects of PAR, VPD, and SWC on the sap flow, respectively. Number and size of the icons indicate the magnitude of the effects.

4.4. Specialized water hydraulic in MOBF

In our study, the partial correlation between MOBF sap flow and environmental factors resembled that of early succession stages, suggesting that the environment of MOBF plays a critical role. This forest experiences a lower VPD yet high PAR intensity (Fig. 4, Tables 1 and 5), a combination aligning with the findings of Zhu et al. [51]. This environmental characteristic may be highly specialized, as Wu et al. [52] reported that *M. breviflora* species exhibit decreased biomass and nutritional productivity at lower altitudes, suggesting a specialization that may not favor growth if MOBF species were moved to lower altitudes.

Such environmental specificities found in MOBF not only underline the unique ecological dynamics within this forest but also enhance our understanding of forest succession across different biomes. The specialized environmental conditions of MOBF - characterized by lower VPD and higher PAR - offer a distinct contrast to typical monsoon evergreen broadleaf forests, providing a pivotal case study in adaptive ecological strategies and resilience. This distinct environment may contribute to a unique microclimate that supports certain physiological adaptations in the resident flora, potentially influencing everything from leaf morphology to root systems. Understanding these adaptations can shed light on the evolutionary pressures that shape forest ecosystems and guide us in predicting their responses to global climate change.

4.5. Limitations

This study has several limitations; first, it only utilized dry season data, and previous research indicates that sap flow responses to microclimate factors can vary between dry and wet seasons, as well as growing and non-growing seasons [12,29]. Moreover, the relationship between the sap flow rate and microclimate factors may differ across time scales [53]. Thus, re-examining on longer scales is necessary to comprehensively understand the interactions between microclimate factors and sap flow dynamics. Another limitation is the exclusive focus on daytime sap flow, while some studies highlight nocturnal sap flow in plants [10,42,54]. However, nocturnal sap flow in S. superba, a dominant tree species in South China, is reportedly smaller than diurnal sap flow [55,56]. Future research should investigate both daytime and nocturnal sap flow better to understand tree water use patterns and responses to microclimate factors.

Additionally, two major limitations should be noted: (1) Climate variables were measured within the canopy, making PAR measurements likely heavily influenced by canopy structure, as evidenced by the very low PAR at MEBF. (2) The experimental design makes it challenging to distinguish elevation effects from forest type/succession effects. Comparisons between MF1 and MF2, as well as MEBF and MOBF, can provide insights into elevation effects since these are similar forest types. For succession effects, comparisons between PF and MF1, as well as MF2 and MEBF, are more appropriate as they grow in similar elevation ranges. The current approach mixes succession and elevation effects, as MEBF is located higher than PF and MF1. Overall, this study provides insight into sap flow dynamics and environmental factor interactions across forest succession stages in subtropical forests. However, future research should examine the multi-dimensional forest ecosystem response to climate change and global warming, such as the impacts of changing precipitation patterns or extreme weather events on sap flow dynamics. This study lays the foundation for further exploring the complex interactions between microclimate factors and sap flow dynamics in subtropical forest ecosystems. Despite the limitations inherent in the study, the research successfully uncovered several interesting insights as followed, underscoring the critical need for further comprehensive research to explore how these nuanced interactions and adaptations influence forest resilience and productivity under changing climatic conditions.

5. Conclusion

The present study elucidates the primary influences on sap flow within the Dinghushan subtropical forest, pinpointing PAR as the predominant driver, with its impact varying significantly across different forest succession stages. A notable delay in sap flow response to PAR was observed, which was more pronounced in late-successional forests, indicating increased sensitivity. As forests progress from early to late succession, the influence of VPD on sap flow diminishes, whereas SWC becomes increasingly predictive of sap flow dynamics. This shift suggests a more complex hydrological adaptation in mature forests, particularly evident in the distinct hydraulic traits of broadleaf species during the transition from middle to late succession stages. These adaptations may reflect broader ecological strategies for coping with environmental stressors associated with climate change.

Acknowledging these findings, it becomes imperative to consider the potential differential impacts of climate change on various forest types. Late-successional forests, with their refined sensitivity to PAR and reliance on SWC, might be more vulnerable to shifts in drought patterns compared to their early-successional counterparts. The study highlights the critical need for further comprehensive research to explore how these nuanced interactions and adaptations influence forest resilience and productivity under changing climatic conditions. This deeper understanding is vital for developing targeted forest management and conservation strategies aimed at mitigating the impacts of global climate change on diverse forest ecosystems.

Data availability

Data will be made available on request.

CRediT authorship contribution statement

Jianqiang Huang: Writing – original draft, Software, Investigation, Data curation. **Fasih Ullah Haider:** Writing – review & editing, Writing – original draft, Validation, Software, Methodology. **Wanxuan Huang:** Methodology, Formal analysis, Data curation. **Shizhong Liu:** Visualization, Software, Data curation. **Brian Njoroge Mwangi:** Writing – review & editing, Software, Investigation. **Vincent Suba:** Methodology, Formal analysis, Data curation. **Lindsay Sikuku:** Software, Methodology, Formal analysis. **Xuli Tang:** Writing – review & editing, Software, Methodology. **Qianmei Zhang:** Writing – review & editing, Formal analysis. **Guowei Chu:** Writing – review & editing, Methodology, Data curation. **Deqiang Zhang:** Writing – original draft, Supervision, Methodology. **Juxiu Liu:** Writing – review & editing, Supervision, Resources. **Ze Meng:** Writing – review & editing, Project administration, Data curation. **Dennis Otieno:** Writing – review & editing, Supervision, Investigation, Conceptualization. **Yuelin Li:** Writing – review & editing, Supervision, Resources, Project administration, Funding acquisition, Conceptualization.

Declaration of competing interest

The authors declare that they have no known competing financial interests or personal relationships that could have appeared to influence the work reported in this paper.

Acknowledgment

This research was supported by the National Natural Science Foundation of China [Grant No. 31961143023]; the National Key Research and Development Program of China [Grant No.2021YFF0703905]; the Dinghushan Forest Ecosystem Positioning Research Station of the National Science and Technology Infrastructure Platform, the Chinese Ecosystem Research Network (CERN); the Science and Technology Program from Forestry Administration of Guangdong Province [2023KYXM09], and the Operation Service Project of the National Scientific Observation and Research Field Station of the Dinghushan Forest Ecosystem of Guangdong, the Ministry of Science and Technology of the People's Republic of China.

Appendix A. Supplementary data

Supplementary data to this article can be found online at https://doi.org/10.1016/j.heliyon.2024.e37530.

References

[1] Q. Yang, X. Zhang, Improving SWAT for simulating water and carbon fluxes of forest ecosystems, Sci. Total Environ. 569–570 (2016) 1478–1488, https://doi.org/10.1016/j.scitotenv.2016.06.238.
[2] S.L. Lewis, D.P. Edwards, D. Galbraith, Increasing human dominance of tropical forests, Science 349 (2015) 827–832, https://doi.org/10.1126/science.aaa9932.
[3] L. Zhou, S. Wang, Y. Chi, W. Ju, K. Huang, R.A. Mickler, M. Wang, Q. Yu, Changes in the carbon and water fluxes of subtropical forest ecosystems in Southwestern China related to drought, Water 10 (2018), https://doi.org/10.3390/w10070821.
[4] G. Zhou, L. Li, Wu Anchi, Effect of drought on forest ecosystem under warming climate, Journal of Nanjing University of Information Science and Technology (Natural Science Edition) 12 (2020) 81–88.
[5] E. Lefi, H. Medrano, J. Cifre, Water uptake dynamics, photosynthesis and water use efficiency in field-grown Medicago arborea and Medicago citrina under prolonged Mediterranean drought conditions, Ann. Appl. Biol. 144 (2004) 299–307.
[6] G. Zhou, C. Peng, Y. Li, S. Liu, Q. Zhang, X. Tang, J. Liu, J. Yan, D. Zhang, G. Chu, A climate change-induced threat to the ecological resilience of a subtropical monsoon evergreen broad-leaved forest in Southern China, Global Change Biol. 19 (2013) 1197–1210, https://doi.org/10.1111/gcb.12128.
[7] A. Verhoef, G. Egea, Modeling plant transpiration under limited soil water: comparison of different plant and soil hydraulic parameterizations and preliminary implications for their use in land surface models, Agric. For. Meteorol. 191 (2014) 22–32, https://doi.org/10.1016/j.agrformet.2014.02.009.
[8] S. Dzikiti, D. Lotter, S. Mpandeli, L. Nhamo, Assessing the energy and water balance dynamics of rain-fed rooibos tea crops (Aspalathus linearis) under changing Mediterranean climatic conditions, Agric. Water Manag. 274 (2022), https://doi.org/10.1016/j.agwat.2022.107944.
[9] M. Hou, F. Tian, S. Ortega-Farias, C. Riveros-Burgos, T. Zhang, A. Lin, Estimation of crop transpiration and its scale effect based on ground and UAV thermal infrared remote sensing images, Eur. J. Agron. 131 (2021) 126389, https://doi.org/10.1016/j.eja.2021.126389.
[10] B. Fan, Z. Liu, K. Xiong, Y. Li, K. Li, X. Yu, Influence of environmental factors on the sap flow activity of the golden pear in the growth period of karst area in southern China, Water 14 (2022) 1707, https://doi.org/10.3390/w14111707.
[11] A. Granier, A new method of sap flow measurement in tree stems, Ann. Sci. For. 42 (1985) 193–200, https://doi.org/10.1051/forest:19850204.
[12] C. Ma, Y. Luo, M. Shao, X. Li, L. Sun, X. Jia, Environmental controls on sap flow in black locust forest in Loess Plateau, China, Sci. Rep. 7 (2017) 13160, https://doi.org/10.1038/s41598-017-13532-8.
[13] D. Otieno, Y. Li, Y. Ou, J. Cheng, S. Liu, X. Tang, Q. Zhang, E. young Jung, D. Zhang, J. Tenhunen, Stand characteristics and water use at two elevations in a subtropical evergreen forest in southern China, Agric. For. Meteorol. 194 (2014) 155–166, https://doi.org/10.1016/j.agrformet.2014.04.002.
[14] W. Liu, Y. Nie, Z. Luo, Z. Wang, L. Huang, F. He, H. Chen, Transpiration rates decline under limited moisture supply along hillslopes in a humid karst terrain, Sci. Total Environ. 894 (2023) 164977, https://doi.org/10.1016/j.scitotenv.2023.164977.
[15] S. Chen, W. Wei, Y. Huang, Biophysical controls on canopy transpiration of *Pinus tabulaeformis* under different soil moisture conditions in the Loess Plateau of China, J. Hydrol. 631 (2024) 130799, https://doi.org/10.1016/j.jhydrol.2024.130799.
[16] Y. Qingjuan, S. Wanyi, L. Ziqi, A microclimate model for plant transpiration effects, Urban Clim. 45 (2022) 101240, https://doi.org/10.1016/j.uclim.2022.101240.
[17] S.M. Vicente-Serrano, D.G. Miralles, N. McDowell, T. Brodribb, F. Domínguez-Castro, R. Leung, A. Koppa, The uncertain role of rising atmospheric CO2 on global plant transpiration, Earth Sci. Rev. 230 (2022) 104055, https://doi.org/10.1016/j.earscirev.2022.104055.
[18] B.D. Bovard, P.S. Curtis, C.S. Vogel, H.-B. Su, H.P. Schmid, Environmental controls on sap flow in a northern hardwood forest, Tree Physiol. 25 (2005) 31–38, https://doi.org/10.1093/treephys/25.1.31.

[19] X. Zhao, P. Zhao, L. Zhu, Q. Wang, Y. Hu, B.M. Cranston, J. Kaplick, O. Lei, X. Chen, G. Ni, Q. Ye, C. Macinnis-Ng, Exploring the influence of biological traits and environmental drivers on water use variations across contrasting forests, Forests 12 (2021), https://doi.org/10.3390/f12020161.
[20] G. Zhou, X. Wei, Y. Wu, S. Liu, Y. Huang, J. Yan, D. Zhang, Q. Zhang, J. Liu, Z. Meng, C. Wang, G. Chu, S. Liu, X. Tang, X. Liu, Quantifying the hydrological responses to climate change in an intact forested small watershed in Southern China, Global Change Biol. 17 (2011) 3736–3746, https://doi.org/10.1111/j.1365-2486.2011.02499.x.
[21] K. Zhao, Y. Wang, R.L. Edwards, H. Cheng, X. Kong, D. Liu, Q. Shao, Y. Cui, C. Huang, Y. Ning, X. Yang, Late Holocene monsoon precipitation changes in southern China and their linkage to Northern Hemisphere temperature, Quat. Sci. Rev. 232 (2020) 106191, https://doi.org/10.1016/j.quascirev.2020.106191.
[22] T. Wu, N. Tan, D.T. Tissue, J. Huang, H. Duan, W. Su, Y. Song, X. Liu, Y. Liu, X. Li, Z. Lie, S. Yang, S. Zhou, J. Yan, X. Tang, S. Liu, G. Chu, X. He, J. Liu, Physiological traits and response strategies of four subtropical tree species exposed to drought, Environ. Exp. Bot. 203 (2022) 105046, https://doi.org/10.1016/j.envexpbot.2022.105046.
[23] Q. Wan, K. Huang, X. Zhang, Y. Yue, H. Peng, T. Ma, X. Yang, Z. Zheng, Regional land cover changes of the last 6,500 years in middle and southern subtropical China, Quat. Int. 641 (2022) 15–24, https://doi.org/10.1016/j.quaint.2022.04.009.
[24] D. Wei, Yang Yang, Ni Xilu, Li Zhigang, Li Long, Regional forest ecosystem services assessment:A case study of ningxia hui autonomous, J. Northwest For. Univ. 33 (2018) 278–284.
[25] Y. Tian, Q. Zhang, X. Liu, Y. Zhang, Time lag effect between stem sap flow and solar radiation in Larch, J. Northeast For. Univ. 46 (2018) 23–26.
[26] L.A. Guillen, E. Brzostek, B. McNeil, N. Raczka, B. Casey, N. Zegre, Sap flow velocities of Acer saccharum and Quercus velutina during drought: insights and implications from a throughfall exclusion experiment in West Virginia, USA, Sci. Total Environ. 850 (2022), https://doi.org/10.1016/j.scitotenv.2022.158029.
[27] C. Körner, Alpine Plant Life: Functional Plant Ecology of High Mountain Ecosystems, Springer International Publishing, Cham, 2021, https://doi.org/10.1007/978-3-030-59538-8.
[28] J. Cheng, X. Ouyang, D. Huang, S. Liu, D. Zhang, Y. Li, Sap flow characteristics of four dominant tree species in a mixed conifer-broadleaf forest in Dinghushan, Acta Ecol. Sin. 35 (2015) 4097–4104.
[29] L. Wang, Deng Yonghong, Zeng Xiaoping, Liu Shizhong, Meng Ze, Li Yuelin, Water use characteristics of pioneer tree Pinus massoniana in south subtropical forest community in China, Journal of Central South University of Forestry & Technology 39 (2019) 82–90.
[30] J. Liu, Li Yuelin, Liu Shizhong, Li Yiyong, Chu Guowei, Meng Ze, Zhang Deqiang, An introduction to an experimental design for studying effects of air temperature rise on model forest ecosystems, Acta Phytoecol. Sin. 37 (2013) 558–565.
[31] W. Huang, L.I.U. Juxiu, T.A.N.G. Xuli, Yuhui Huang, L.I.U. Shizhong, C.H.U. Guowei, Z.H.O.U. Gouyi, Inorganic nitrogen and available phosphorus concentrations in the soils of five forests at dinghushan, China, Chin. J. Appl. Environ. Biol. 15 (2009) 441–447.
[32] S. Liu, L.U.O. Yan, H.U.A.N.G. Yuhui, Z.H.O.U. Guoy, Studies on the community biomass and its allocations of five forest types in Dinghushan Nature Reserve, Ecologic Science 26 (2007) 387–393.
[33] D. Zhang, W. Ye, Q. Yu, G. Sun, Y. Zhang, The litter-fall of representative forests of successional series in Dinghushan, Acta Ecol. Sin. 20 (2000) 938–944.
[34] G.S. Campbell, J.M. Norman, An Introduction to Environmental Biophysics, Springer, New York, NY, 1998, https://doi.org/10.1007/978-1-4612-1626-1.
[35] A. Granier, Evaluation of transpiration in a Douglas-fir stand by means of sap flow measurements, Tree Physiol. 3 (1987) 309–320, https://doi.org/10.1093/treephys/3.4.309.
[36] Q. Wang, A. Lintunen, P. Zhao, W. Shen, Y. Salmon, X. Chen, L. Ouyang, L. Zhu, G. Ni, D. Sun, X. Rao, T. Hölttä, Assessing environmental control of sap flux of three tree species plantations in degraded hilly lands in South China, Forests 11 (2020) 206, https://doi.org/10.3390/f11020206.
[37] C. Pappas, A.M. Matheny, J.L. Baltzer, A.G. Barr, T.A. Black, G. Bohrer, M. Detto, J. Maillet, A. Roy, O. Sonnentag, J. Stephens, Boreal tree hydrodynamics: asynchronous, diverging, yet complementary, Tree Physiol. 38 (2018) 953–964, https://doi.org/10.1093/treephys/tpy043.
[38] A.C. Oishi, D.A. Hawthorne, R. Oren, Baseliner: an open-source, interactive tool for processing sap flux data from thermal dissipation probes, SoftwareX 5 (2016) 139–143, https://doi.org/10.1016/j.softx.2016.07.003.
[39] R Core Team, R, A language and environment for statistical computing. https://www.R-project.org/, 2020.
[40] M. Hlavac, Stargazer: well-formatted regression and summary statistics tables. https://CRAN.R-project.org/package=stargazer, 2021.
[41] Y. Tan, C. Zhan, H. Yang, Z. Xiao, J. Peng, Communities in Nan'ao Island, Guangdong Province inter-specific associations among main tree species in Machilus chinensis communities in Nan'ao Island, Journal of Central South University of Forestry & Technology 32 (2012) 92–99. Guangdong Province.
[42] P. Wu, Liu Yunqiang, Li Dongmei, Zhijun Chen, Ma Changming, Driving influence of environmental factors on the sap flow of the artificial poplar forest on sandy land, Chin. J. Agrometeorol. 42 (2021) 402–411.
[43] S. Ding, L.U. XunLing, L.I. HaoMin, A comparison of light environmental characteristics for evergreen broad-leaved forest communities from different successional stages in Tiantong National Forest Park, Acta Ecol. Sin. 25 (2005) 2862–2867.
[44] L. Wang, Hu Yanting, Deqiang Zhang, Shizhong Liu, Meng Ze, Otieno Dennis, Li Yuelin, Ozone uptake by the dominant canopy tree species in a natural mixed coniferbroadleaf forest in Dinghushan,Guangdong Province,south China, Acta Ecol. Sin. 38 (2018) 6092–6100.
[45] Q. Tie, H. Hu, F. Tian, H. Guan, H. Lin, Environmental and physiological controls on sap flow in a subhumid mountainous catchment in North China, Agric. For. Meteorol. (2017) 240–241, https://doi.org/10.1016/j.agrformet.2017.03.018, 46–57.
[46] C.W. Berish, Root biomass and surface area in three successional tropical forests, Can. J. For. Res. 12 (1982) 699–704, https://doi.org/10.1139/x82-104.
[47] S.M. Uselman, R.G. Qualls, J. Lilienfein, Fine root production across a primary successional ecosystem chronosequence at Mt. Shasta, California, Ecosystems 10 (2007) 703–717, https://doi.org/10.1007/s10021-007-9045-8.
[48] P. Wu, W. Yang, Y. Cui, W. Zhao, D. Shu, Y. Hou, F. Ding, Characteristics of sap flow and correlation analysis with environmental factors of Acer wangchii in the karst area, Acta Ecol. Sin. 37 (2017) 7552–7567.
[49] W. Fang, N. Lu, Y. Zhang, L. Jiao, B. Fu, Responses of nighttime sap flow to atmospheric and soil dryness and its potential roles for shrubs on the Loess Plateau of China, J. Plant Ecol. 11 (2018) 717–729, https://doi.org/10.1093/jpe/rtx042.
[50] N. Obojes, E. Tasser, C. Newesely, S. Mayr, U. Tappeiner, in: T. Holtta, Y. Salmon (Eds.), Comparing Sap Flow of European Larch with Evergreen Conifers at Different Elevations in an Inner-Alpine Dry Valley, 2020, pp. 113–120, https://doi.org/10.17660/ActaHortic.2020.1300.15.
[51] L. Zhu, Y. Zhang, H. Ye, Y. Li, W. Hu, J. Du, P. Zhao, Variations in leaf and stem traits across two elevations in subtropical forests, Funct. Plant Biol. 49 (2022) 319–332, https://doi.org/10.1071/FP21220.
[52] T. Wu, S. Liu, Z. Lie, M. Zheng, H. Duan, G. Chu, Z. Meng, G. Zhou, J. Liu, Divergent effects of a 6-year warming experiment on the nutrient productivities of subtropical tree species, For. Ecol. Manag. 461 (2020), https://doi.org/10.1016/j.foreco.2020.117952.
[53] J. Zhang, L. Wang, X. Han, L. Zhang, The relationship between sap flow velocity and environmental factors of the 19 a apple trees on the loess plateau at different time scales, Sci. Agric. Sin. 49 (2016) 2583–2592.
[54] Y. Su, X. Wang, Y. Sun, H. Wu, Sap flow velocity in fraxinus pennsylvanica in response to water stress and microclimatic variables, Front. Plant Sci. 13 (2022) 884526, https://doi.org/10.3389/fpls.2022.884526.
[55] C. Zhou, P. Zhao, G. Ni, Q. Wang, X. Zeng, Z. Li-wei, X. Cai, Water recharge through nighttime stem sap flow of Schima superba in Guangzhou region of Guangdong Province, South China: affecting factors and contribution to transpiration, Yingyong Shengtai Xuebao 23 (2012) 1751–1757.
[56] X. Zhao, Ping Zhao, L. Zhu, Differentiating refilling and transpiration from night-time sap flux based on time series modelling, Trees Struct. Funct. 36 (2022) 1621–1632, https://doi.org/10.1007/s00468-022-02316-x.
[57] E. Gerzon, I. Biton, Y. Yaniv, H. Zemach, Y. Netzer, A. Schwartz, A. Fait, G. Ben-Ari, Grapevine anatomy as a possible determinant of isohydric or anisohydric behavior, Am. J. Enol. Vitic. 66 (2015) 340–347, https://doi.org/10.5344/ajev.2015.14090.

[58] J.-M. Limousin, C.P. Bickford, L.T. Dickman, R.E. Pangle, P.J. Hudson, A.L. Boutz, N. Gehres, J.L. Osuna, W.T. Pockman, N.G. Mcdowell, Regulation and acclimation of leaf gas exchange in a piñon–juniper woodland exposed to three different precipitation regimes, Plant Cell Environ. 36 (2013) 1812–1825, https://doi.org/10.1111/pce.12089.

[59] A. Kume, Importance of the green color, absorption gradient, and spectral absorption of chloroplasts for the radiative energy balance of leaves, J. Plant Res. 130 (2017) 501–514, https://doi.org/10.1007/s10265-017-0910-z.

[60] S. Li, L. Fang, J.N. Hegelund, F. Liu, Elevated CO2 modulates plant hydraulic conductance through regulation of PIPs under progressive soil drying in tomato plants, Front. Plant Sci. 12 (2021) 666066, https://doi.org/10.3389/fpls.2021.666066.